

# Linear assembly of two-patch silica nanoparticles and control of chain length by coassembly with colloidal chain stoppers

Bin Liu<sup>†,‡</sup>, Weiya Li<sup>†,‡</sup>, Etienne Duguet<sup>‡</sup>, and Serge Ravaine<sup>†,\*</sup>

<sup>†</sup>Univ. Bordeaux, CNRS, CRPP, UMR 5031, F-33600 Pessac, France

<sup>‡</sup>Univ. Bordeaux, CNRS, Bordeaux INP, ICMCB, UMR 5026, F-33600 Pessac, France

KEYWORDS. Colloidal polymers; Nanoparticles; Patchy; Self-assembly; Chain stoppers

---

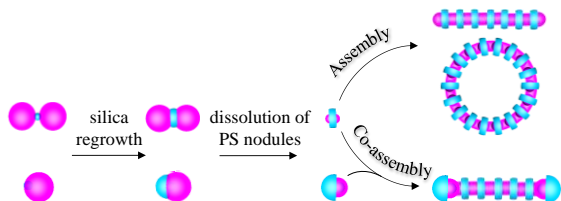
**ABSTRACT:** Self-assembly of patchy nano-sized building blocks is an efficient strategy for producing highly organized materials. Herein, we report the chaining of divalent silica nanoparticles with polystyrene patches dispersed in THF triggered by lowering the solvent quality. We study the influence of the patch-to-particle size ratio and show that the nature of the added nonsolvent, *e.g.* ethanol, water or salty water, and its volume fraction shall be carefully adjusted. We demonstrate that colloidal assembly initially obeys the kinetic model of step-growth polymerization and that beyond a certain length the chains have the possibility to cyclize. We also show that the length of the chains can be controlled by the addition of one-patch silica nanoparticles, which act as colloidal analogues of chain stoppers.

---

Chaining of particles, also described as colloidal polymerization, is a field of intense research<sup>1-3</sup> that was recently reviewed several times.<sup>4-7</sup> It was reported that patchy particles are good candidates for acting as colloidal monomers and for promoting the directional assembly of one-dimensional structures.<sup>8-11</sup> For instance, the assembly of Janus particles with one face selectively functionalized with DNA having self-complementary sticky end led to the formation of colloidal chains at different patch ratios.<sup>12</sup> Nguyen *et al.* assemble two-patch particles into polymers using Casimir forces and nicely showed that starting from a water-rich solvent gave rise to an attractive force between the hydrophilic cores of the particles forming a ladder type polymer.<sup>13</sup> On the contrary, an organic-rich solvent promoted the hydrophobic interaction between the patches, forming linear chains. The regioselective binding of cetyltrimethylammonium bromide molecules along the lateral facets of gold nanorods and bipyramids has also extensively been exploited to bind functional derivatives onto the terminal facets of the nanoparticles in order to promote chain formation.<sup>14-20</sup> By adding water to a dimethylformamide suspension of gold nanorods whose tips were functionalized with thiol-terminated polystyrene (PS) oligomers, Nie *et al.* reduced the solubility of PS, thereby triggering nanorod assembly in chains.<sup>19</sup> The same group also performed a quantitative study of the assembly process in order to predict the chain topology and the kinetics of the chain growth.<sup>21-23</sup> The colloidal polymerization was shown to follow a step-growth polymerization model, the nanorods acting as multifunctional monomers and forming reversible, noncovalent bonds at specific bond angles. The quantitative fine-tuning of the assembled structures was further achieved by polymerizing PS-terminated gold nanorods in

the presence of Au-Fe<sub>3</sub>O<sub>4</sub> heterodimers acting as monofunctional colloidal chain stoppers.<sup>24</sup> Nevertheless, the synthesis of colloidal polymer systems with a good control over fundamental structural features such as chain length, composition, and architecture remains challenging nowadays. We recently reported the formation of colloidal polymers through the solvent-induced assembly of two-patch silica nanoparticles (2-PSN).<sup>25</sup> Herein, we investigate for the first time the assembly behavior of 2-PSN with different patch-to-particle size ratios and we show that chaining strongly depends on the composition of the solvent mixture employed during the incubation. Our approach comprises three main steps (Scheme 1): synthesis of binary silica/PS bipods by emulsion polymerization; precise regrowth of the silica core of the obtained bipods and dissolution of their PS nodules to form 2-PSN with a well-defined morphology; fine tuning of the solvent composition to promote their polymerization. We also address the challenging question of the achievement of a predetermined chain length, which was only possible by quenching the assembly after an appropriate time.<sup>25</sup> We demonstrate that one-patch silica nanoparticles (1-PSN) can act as chain stoppers to finely tune the colloidal chain length (Scheme 1, bottom row), as the chains tend to be shorter when the amount of chain stoppers increases.

**Scheme 1. Solvent-induced assembly of divalent silica nanoparticles and their co-assembly with one-patch chain stoppers.**



We first synthesized PS/silica bipods with a morphological yield of 97 % (Figure S1) by seeded emulsion polymerization, as reported elsewhere.<sup>26</sup> Through the addition of a precise volume of tetraethoxysilane (TEOS), we regrew the silica core of the bipods until a predefined diameter (Figure 1, top row and Figure S2). The subsequent dissolution of the PS nodules in tetrahydrofuran (THF) gave rise to disc-like silica nanoparticles with some polymer chains which remain grafted on their faces,<sup>27-28</sup> forming organic bumps (Figure 1, bottom row and Figure S4).

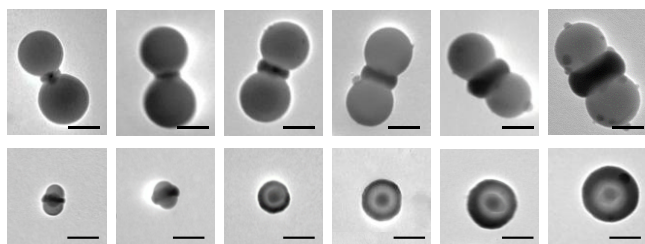


**Figure 1.** TEM images of the bipods obtained after addition of (from left to right): 30  $\mu\text{L}$ , 55  $\mu\text{L}$ , 70  $\mu\text{L}$ , 115  $\mu\text{L}$ , 400  $\mu\text{L}$  and 500  $\mu\text{L}$  of TEOS (top row) and of the corresponding 2-PSN with  $D = 65$  nm, 85 nm, 105 nm, 130 nm, 155 nm and 190 nm, respectively, obtained after dissolution of the PS lobes (bottom row). Scale bars: 100 nm.

We previously showed that we assembled 155-nm and 190-nm 2-PSN in chains by adding 30 vol.% of salty water into the NPs dispersion in THF, thereby reducing both the electrostatic repulsions between NPs due to negatively

charged silanolate groups at their surface and solvent quality for the PS chains (Figure 2e-f and Figure S6).<sup>25</sup> Similar results were obtained when changing the salty water concentration, as shown in Figure 2i. We thus decided to investigate the behavior of the 2-PSN with smaller sizes by adding salty water as bad solvent for the PS chains. We observed the formation of chains when using 130-nm 2-PSN, but uncontrolled aggregation of the 2-PSN with smaller sizes systematically occurred (Figure 2i). Since the formation of a particular structure (aggregates, chains) is governed by the interplay of poor solvency attractions between the PS chains and electrostatic repulsions between the 2-PSN, we speculated that the formation of aggregates is governed by the combination of two factors due the small size of the 2-PSN: first the reduction of the electrostatic repulsive interactions as the silica surface area is small and secondly the greater propensity of the grafted PS chains to interact in all directions as they are less confined at the bottom of the cavities of the 2-PSN. In order to verify this assumption, we performed another series of experiments by using only pure water as bad solvent for the PS grafts in order to avoid screening of the electrostatic repulsions between the 2-PSN. Figure 2h shows that the addition of small amount of water (1 % or 10 %) allowed the formation of chains from 85-nm, 105-nm and 130-nm 2-PSN (Figure 2d), while chaining of the large monomers (155 nm and 190 nm) was not possible anymore, probably because of the too strong electrostatic repulsions between them. It should be noted that assembly experiments performed with 65-nm 2-PSN in pure and salty water led to poorly reproducible results. We assumed that it was due to their dissolution, which is particularly deleterious considering their small size, as many

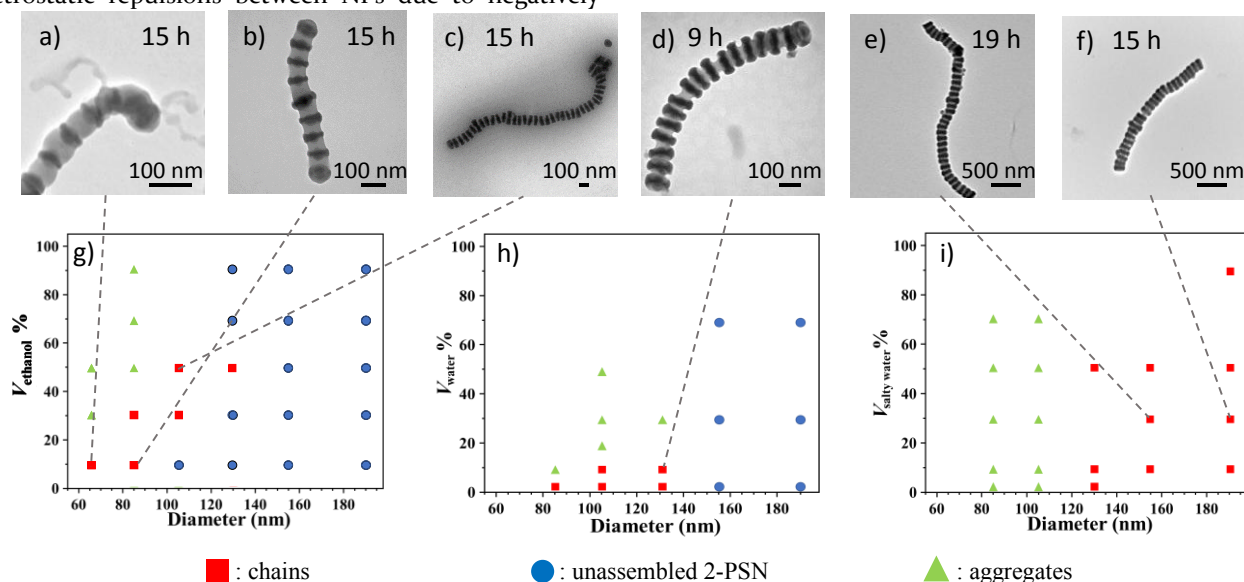


**Figure 2.** a-f) Representative TEM images of chains obtained after incubating 2-PSN for the indicated duration in a THF/ethanol, THF/water or THF/salty water mixture. Phase diagrams identifying the main products of self-assembly as a function of the 2-PSN diameter in different solvent mixtures: g) THF/ethanol; h) THF/water and i) THF/salty water.

partially etched nanoparticles could be observed. A third series of experiments was thus conducted by replacing water with ethanol. Figures 2a-c and 2g show that chaining of 2-PSN as small as 65 nm occurred when adding ethanol into the dispersions of 2-PSN in THF. In all cases, depolymerization of the chains leading to a complete recovery of free 2-PSN occurred within few seconds after the addition of THF.

A detailed study of the assembly of the 105-nm and 130-nm 2-PSN occurring in the 1/1 THF/ethanol and 9/1 THF/water mixtures, respectively, showed the formation of ring-like structures (Figures 3a-b). A statistical analysis of TEM pictures show that ~20 % of the chains enclosed to form rings. Moreover, Figure 3c shows that rings generally contain more 2-PSN monomer units than chains. Such a behavior can be explained by the fact that short chains were too stiff to bend. When the chains became long enough, they could enclose to form rings. More precisely, rings contain systematically at least ten 2-PSN monomers units. This degree of polymerization would thus correspond to the critical length from which the cyclization is possible; it seems moreover little sensitive to the diameter of the 2-PSN.

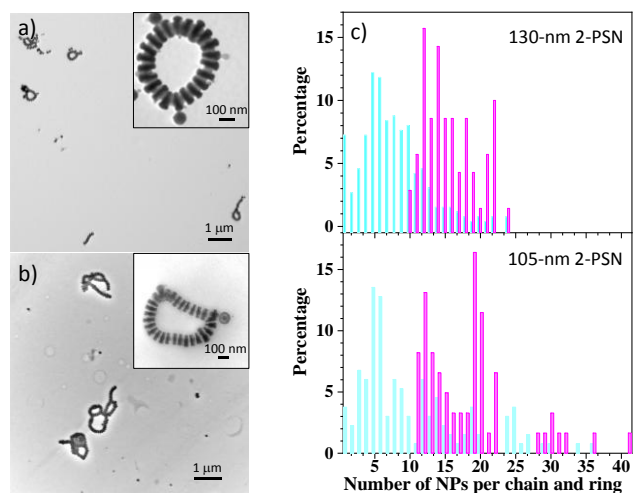


**Figure 3.** TEM images of rings obtained after incubating: a) 130-nm 2-PSN in a 9/1 (vol/vol) THF/water mixture for 63 hours. b) 105-nm 2-PSN in a 1/1 (vol/vol) THF/ethanol for 15 hours. c) Distribution of the number of 2-PSN monomer units per chain (light blue) and ring (magenta).

The kinetics of the chaining of the 105-nm and 130-nm 2-PSN was studied by performing statistical analysis of the TEM images recorded at different assembly times. We measured the number-average degree of polymerization,  $\bar{X}_n$ , defined as:  $\bar{X}_n = \frac{\sum n_x x}{\sum n_x}$ , where  $x$  is the number of 2-PSN in the chain and  $n_x$  is the number of chains containing  $x$  2-PSN. The unassembled 2-PSN were included in

the calculations. Figure 4a shows the evolution of  $\bar{X}_n$  with time. For assembly time shorter than ~5 h, the measured  $\bar{X}_n$  grows linearly with time, which is characteristic of molecular step-growth polymerization. Following the rate equation for the externally catalyzed polymerization of bifunctional monomers with identical functional end groups,  $\bar{X}_n = 2 [M_0]kt + 1$ ,<sup>29</sup> where  $[M_0]$  is the initial concentration of 2-PSN and  $t$  is the assembly time, we calculated the polymerization rate constant  $k$  from the linear fitting of  $\bar{X}_n \sim t$  curves. We found that  $k = 3.77 \cdot 10^5 \text{ L} \cdot \text{mol}^{-1} \cdot \text{s}^{-1}$  and  $1.80 \cdot 10^5 \text{ L} \cdot \text{mol}^{-1} \cdot \text{s}^{-1}$  for the polymerization of 105-nm and 130-nm 2-PSN, respectively. These values are of the same order of magnitude as that found for the chains obtained from 190-nm 2-PSN<sup>25</sup> and for the copolymerization of inorganic nanoparticles.<sup>2</sup> At longer times ( $t > 5$  h),  $\bar{X}_n$  does not vary linearly with time anymore (Figure 4a). The polymerization of 2-PSN seems to follow a different pathway, that is, most likely, a “diffusion-controlled” stage, which can be possibly attributed to the fact that the cyclization of the chains or their sedimentation becomes the rate-limiting factor when they become relatively long. This has been confirmed by the calculation of the polydispersity index of the chains, PDI, which is defined as  $PDI = \bar{X}_w / \bar{X}_n$ , where  $\bar{X}_w = \frac{\sum n_x x^2}{\sum n_x x}$  is the weight-average degree of polymerization, as it was found to be smaller than the value predicted by Flory’s model (*i.e.*  $PDI = 2 - 1/\bar{X}_n$ ) for both sizes of 2-PSN (Figure S7).

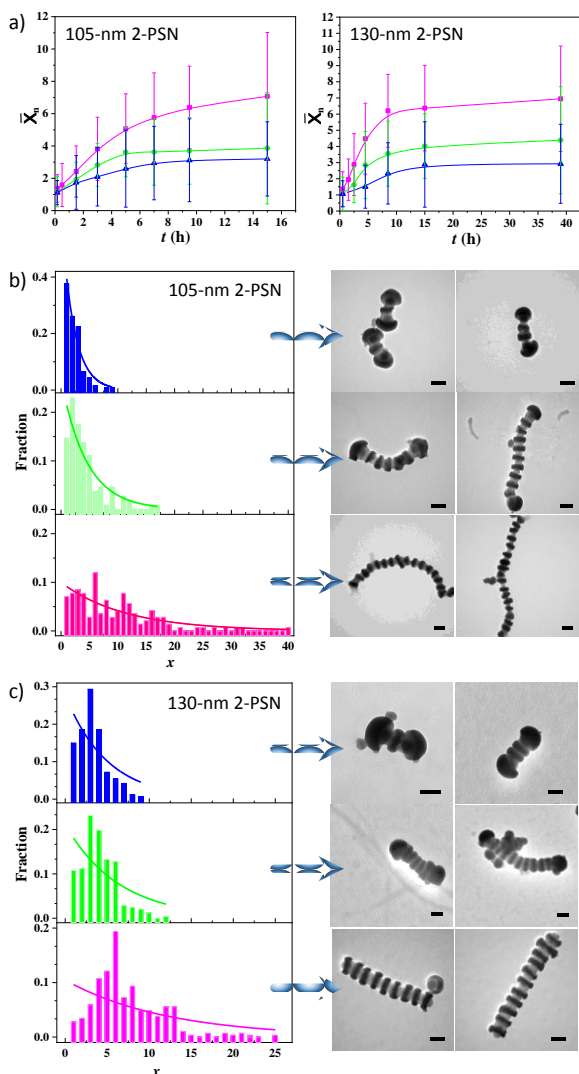


**Figure 4.** a) Dependency of  $\bar{X}_n$  on time for  $[1\text{-PSN}]/[2\text{-PSN}] = 0$  (magenta), 0.25 (green) and 0.5 (blue). Error bars indicate standard deviations of counting. b-c) Distribution of the chain length and representative TEM pictures of chains for  $[1\text{-PSN}]/[2\text{-PSN}] = 0$  (magenta), 0.25 (green) and 0.5 (blue) at  $t = 15$  h. Scale bars: 100 nm. Curves are a guide to the eye.

It was previously shown that the addition of monofunctional “stoppers” into suspensions of soft patchy nanoparticles<sup>30</sup>, gold nanorods<sup>24</sup> or silver nanoplates<sup>3</sup> allowed the control of chain length. In this context, we synthesized 1-PSN by following the previously described synthetic pathway and by using PS/silica monopods (Figure S1) as precursors. Figure S5 shows that 1-PSN have an acorn-like morphology, in which the spherical silica seed is capped by a thin PS shell of about 20 nm corresponding to covalently grafted macromolecules that could not be dissolved in THF.<sup>27</sup> We used these nanoparticles as colloidal chain stoppers by introducing them to the suspension of 2-PSN at the ratio  $0 \leq [1\text{-PSN}]/[2\text{-PSN}] \leq 0.5$ , where  $[1\text{-PSN}]$  and  $[2\text{-PSN}]$  are the molar concentrations of 1-PSN and 2-PSN, respectively. Figure 4a–c summarizes the

dependence of the length distribution of the co-assemblies on the mixing ratio  $[1\text{-PSN}]/[2\text{-PSN}]$ . The decrease in mean chain length when this ratio increases is evident when comparing the TEM images taken at  $t = 15$  h. Figure 4a shows that the addition of a particular amount of 1-PSN allows one to fine-tune the length of the colloidal polymers at a particular self-assembly time. For instance, for  $t = 7$  h, the average number of 105-nm 2-PSN in the chains is 5.76 in the absence of 1-PSN, whereas it is only equal to 2.95 at the ratio  $[1\text{-PSN}]/[2\text{-PSN}] = 0.5$ .

In summary, this work shows that 2-PSN with different patch-to-particle size ratio can polymerize to form chains through a fine-tuning of the solvent mixture composition. The colloidal polymerization follows a two-stage process, involving step-growth polymerization at short assembly time and diffusion-controlled polymerization at longer ones. The introduction of one-patch nanoparticles acting as colloidal chain stoppers at the beginning of the self-assembly enables us to control the chain length. We anticipate these results open up avenues to construct new colloidal analogues of one-dimensional structures found in nature. For instance, the inherent flexibility of the chains of 2-PSN resulting from the length of the PS macromolecules acting as bridges enables us to envision the preparation of folding colloidal analogues of biopolymers.

## ASSOCIATED CONTENT

**Supporting Information.** This material is available free of charge via the Internet at <http://pubs.acs.org>.

Materials, synthesis and characterization of patchy nanoparticles. TEM images of monopods, bipods, patchy silica NPs and low-magnification TEM images of chains assembled from these patchy NPs.

## AUTHOR INFORMATION

### Corresponding Author

Prof. Serge Ravaine – Centre de Recherche Paul Pascal, 115 avenue du Dr A. Schweitzer 33600 Pessac, France.  
 orcid.org/0000-0002-6343-8793.  
 Email : serge.ravaine@crpp.cnrs.fr

### Author Contributions

The project was supervised by E.D. and S.R. Nanoparticle synthesis and assembly experiments were conducted by B.L. and W.L. All authors have given approval to the final version of the manuscript.

## ACKNOWLEDGMENT

B. Liu and W. Li were supported by a grant from the China Scholarship Council.

## REFERENCES

- (1) Gu, M.; Ma, X.; Zhang, L.; Lin, J. Reversible polymerization-like kinetics for programmable self-assembly of DNA-encoded nanoparticles with limited valence. *J. Am. Chem. Soc.* **2019**, *141*, 16408–16415.

- (2) Yi, C.; Yang, Y.; Nie, Z. Alternating copolymerization of inorganic nanoparticles. *J. Am. Chem. Soc.* **2019**, *141*, 7917–7925.
- (3) Luo, B.; Smith, J. W.; Wu, Z.; Kim, J.; Ou, Z.; Chen, Q. Polymerization-like co-assembly of silver nanoplates and patchy spheres. *ACS Nano* **2017**, *11*, 7626–7633.
- (4) Velev, O. D.; Gupta, S. Materials fabricated by micro- and nanoparticle assembly – the challenging path from science to engineering. *Adv. Mater.* **2009**, *21*, 1897–1905.
- (5) Liu, K.; Zhao, N.; Kumacheva, E. Self-assembly of inorganic nanorods. *Chem. Soc. Rev.* **2011**, *40*, 656–671.
- (6) Hill, L. J.; Pinna, N.; Char, K.; Pyun, J. Colloidal polymers from inorganic nanoparticle monomers. *Prog. Polym. Sci.* **2015**, *40*, 85–120.
- (7) Cademartiri, L.; Bishop, K. J. M. Programmable self-assembly. *Nat. Mater.* **2015**, *14*, 2–9.
- (8) Coluzza, I.; van Oostrum, P. D. J.; Capone, B.; Reimhult, E.; Dellago, C. Design and folding of colloidal patchy polymers. *Soft Matter* **2013**, *9*, 938–944.
- (9) Onishi, S.; Tokuda, M.; Suzuki, T.; Minami, H. Preparation of Janus particles with different stabilizers and formation of one-dimensional particle arrays. *Langmuir* **2015**, *31*, 674–678.
- (10) Tigges, T.; Walther, A. Hierarchical self-assembly of 3D-printed lock-and-key colloids through shape recognition. *Angew. Chemie Int. Ed.* **2016**, *55*, 11261–11265.
- (11) Zhao, S.; Wu, Y.; Lu, W.; Liu, B. Capillary force driving directional 1D assembly of patchy colloidal discs. *ACS Macro Letters* **2019**, *8*, 363–367.
- (12) Oh, J. S.; Lee, S.; Glotzer, S. C.; Yi, G.-R.; Pine, D.J. Colloidal fibers and rings by cooperative assembly. *Nat. Commun.* **2019**, *10*, 3936.
- (13) Nguyen, T. A.; Newton, A.; Veen, S. J.; Kraft, D. J.; Bolhuis, P. G.; Schall, P. Switching colloidal superstructures by critical Casimir forces. *Adv. Mater.* **2017**, *29*, 1700819.
- (14) Caswell, K. K.; Wilson, J. N.; Bunz, U. H. F.; Murphy, C. J. Preferential end-to-end assembly of gold nanorods by biotin-streptavidin connectors. *J. Am. Chem. Soc.* **2003**, *125*, 13914–13915.
- (15) Sau, T. K.; Murphy, C. J. Self-assembly patterns formed upon solvent evaporation of aqueous cetyltrimethylammonium bromide-coated gold nanoparticles of various shapes. *Langmuir* **2005**, *21*, 2923–2929.
- (16) Zhang, S.; Kou, X.; Yang, Z.; Shi, Q.; Stucky, G. D.; Sun, L.; Wang, J.; Yan, C. Nanonecklaces assembled from gold rods, spheres, and bipyramids. *Chem. Commun.* **2007**, 1816–1818.
- (17) Park, H. S.; Agarwal, A.; Kotov, N. A.; Lavrentovich, O. D. Controllable side-by-side and end-to-end assembly of Au nanorods by lyotropic chromonic materials. *Langmuir* **2008**, *24*, 13833–13837.
- (18) Pan, B.; Ao, L.; Gao, F.; Tian, H.; He, R.; Cui, D. End-to-end self-assembly and colorimetric characterization of gold nanorods and nanospheres via oligonucleotide hybridization. *Nanotechnology* **2005**, *16*, 1776–1780.
- (19) Nie, Z.; Fava, D.; Kumacheva, E.; Zou, S.; Walker, G. C.; Rubinstein, M. Self-assembly of metal-polymer analogues of amphiphilic triblock copolymers. *Nature Mater.* **2007**, *6*, 609–614.
- (20) Fava, D.; Nie, Z.; Winnik, M. A.; Kumacheva, E. Evolution of self-assembled structures of polymer-terminated gold nanorods in selective solvents. *Adv. Mater.* **2008**, *20*, 4318–4322.
- (21) Liu, K.; Lukach, A.; Sugikawa, K.; Chung, S.; Vickery, J.; Therien-Aubin, H.; Yang, B.; Rubinstein, M.; Kumacheva, E. Copolymerization of metal nanoparticles: A route to colloidal plasmonic copolymers. *Angew. Chemie Int. Ed.* **2014**, *53*, 2648–2653.
- (22) Liu, K.; Nie, Z.; Zhao, N.; Li, W.; Rubinstein, M.; Kumacheva, E. Step-growth polymerization of inorganic nanoparticles. *Science* **2010**, *329*, 197–200.
- (23) Liu, K.; Resetco, C.; Kumacheva, E. Salt-mediated kinetics of the self-assembly of gold nanorods end-tethered with polymer ligands. *Nanoscale* **2012**, *4*, 6574–6580.
- (24) Klinkova, A.; Therien-Aubin, H.; Choueiri, R. M.; Rubinstein, M.; Kumacheva, E. Colloidal analogs of molecular chain stoppers. *Proc. Natl. Acad. Sci.* **2013**, *110*, 18775–18779.
- (25) Li, W.; Liu, B.; Hubert, C.; Perro, A.; Duguet, E.; Ravaine, S. Self-assembly of colloidal polymers from two-patch silica nanoparticles. *Nano Res.* **2020**, *13*, 3371–3376.
- (26) Désert, A.; Morele, J.; Taveau, J. C.; Lambert, O.; Lansalot, M.; Bourgeat-Lami, E.; Thill, A.; Spalla, O.; Belloni L.; Ravaine S.; Duguet, E. Multipod-like silica/polystyrene clusters. *Nanoscale* **2016**, *8*, 5454–5469.
- (27) Hubert, C.; Chomette, C.; Désert, A.; Sun, M.; Tréguer-Delapierre, M.; Mornet, S.; Perro, A.; Duguet, E.; Ravaine, S. Synthesis of multivalent silica nanoparticles combining both enthalpic and entropic patchiness. *Faraday Discuss.* **2015**, *181*, 139–146.
- (28) Chomette, C.; Duguet, E.; Mornet, S.; Yammine, E.; Manoharan, V. N.; Schade, N. B.; Hubert, C.; Ravaine, S.; Perro, A.; Treguer-Delapierre, M. Templated growth of gold satellites on dimpled silica cores. *Faraday Discuss.* **2016**, *191*, 105–116.
- (29) Flory, P. Principles of polymer chemistry; Cornell University Press Ed., 1953.
- (30) Gröschel, A.; Walther, A.; Löbbling, T. I.; Schacher, F. H.; Schmalz, H.; Müller, A. H. E. Guided hierarchical co-assembly of soft patchy nanoparticles. *Nature* **2013**, *503*, 247–251.

# Table of Contents artwork

